Bulletin of the Seismological Society of America, Vol. 98, No. 4, pp. 1863–1875, August 2008, doi: 10.1785/0120070172

Empirical Relationships between Modified Mercalli Intensity and Engineering Ground-Motion Parameters in Greece

by G-Akis Tselentis and Laurentiu Danciu

Abstract New relationships between modified Mercalli intensity (MMI) and engineering ground-motion parameters are developed for Greece. The ground-motion parameters investigated were peak ground acceleration (PGA), velocity, displacement, Arias intensity, and cumulative absolute velocity. The observed earthquake intensity is quantified in terms of the observed MMI at the recording station and the data set consists of 310 time histories recorded from 89 Greek earthquakes. The selected records were found to be characterized by high-frequency, low-energy content and short duration. Two sets of empirical relationships between MMI and the selected ground-motion parameters were derived. The first set of MMI predictive equations are independent of magnitude and epicentral distance, and they were derived by fitting the mean values of the ground-motion parameters using a weighted least-squares regression technique. The influence of magnitude, epicentral distance, and the local site conditions were incorporated into the second MMI predictive model, resulting in a decrease of the model variance. The lowest standard deviation observed for the first MMI predictive model was for PGA, while for the second MMI predictive model, Arias intensity exhibited the smallest variability. Another finding of the present study was that the local site effect has a little influence on the MMI predictive model for peak ground velocity (PGV). The proposed predictive equations are valid for MMI values IV–VIII, and some of them might be used for rapid assessment of the ground shaking and mapping damage potential.

Introduction

Various macroseismic intensity scales have been developed to quantify the severity of the ground shaking on the basis of observed or felt effects in a limited area. Macroseismic intensity scales are subject to interpretation, due to the wide variation of geological conditions, the response of the structures, the uncertainty related to the construction's condition before the earthquake, the type of construction, and the density of population.

Macroseismic intensity is useful because it provides information for preinstrumental earthquakes. However, a physically based ground-motion measure is needed for engineering purposes. With the advent of instrumental seismology, the correlation between the felt intensity with ground-motion parameters has become a topic of increasing interest. This offers the possibility of transforming readily observed data (intensity) into widely used parameters that are useful for engineering purposes (engineering ground-motion measures), to evaluate the historical earthquakes for which no instrumental data are available, to assess seismic hazard and damages, to correlate different intensity scales, and to rapidly assess the severity of ground shaking (Wald, Quintoriano, Heaton, Kanamori, Scrivner, *et al.*, 1999).

Until recently, the macroseismic intensity was related most frequently to peak ground acceleration (PGA) because that parameter is important for seismic resistant design, as the product of PGA and mass represents the inertial force loading the structures (Gutenberg and Richter, 1956; Hershberger, 1956; Ambraseys, 1974; Murphy and O'Brien, 1977; McCann *et al.*, 1980; Krinitzsky and Chang, 1988). In recent years, research on earthquake damage prediction has concluded that some other ground-motion characteristics such as duration, frequency, and energy content all contribute to the structural damage.

Focusing either on regional or worldwide data, many empirical equations have been proposed to relate the felt intensity with peak ground velocity (PGV) (Panza *et al.*, 1997; Wald, Quitoriano, Heaton, Kanamori, 1999; Wu *et al.*, 2003; Kaka and Atkinson, 2004; Atkinson and Kaka, 2007;Kaka and Atkinson, 2007), duration of ground motion (Trifunac and Westermo, 1977), response spectra (Kaka and Atkinson, 2007), Fourier spectra (Sokolov, 1998, 2002), cumulative absolute velocity (CAV) (Cabanas *et al.*, 1997; Kostov, 2005), Arias intensity (I_a) (Margottini *et al.*, 1992), Housner's spectrum intensity, and Japan Meteorological Agency instrumental intensity (Karim and Yamazaki, 2002).

Previous work in Greece was conducted by Koliopoulos *et al.* (1998), who derived empirical regression equations for modified Mercalli intensity (MMI) and various ground-motion parameters such as duration, CAV, I_a, characteristic intensity, Housner's spectrum intensity, and total elastic input energy index.

The main goals of the present study are two: (1) to investigate the relationship between duration and energy characteristics of the Greek strong ground-motion data and (2) to analyze the degree of correlation between the selected ground-motion parameters and the observed intensity. An attempt is made to correlate the felt intensity information with the engineering ground-motion parameters derived from strong-motion data recorded in Greece. Structural damage is a complex function of the ground-motion and structural response, and several ground-motion parameters have been investigated. The parameters of interest in the present investigation are PGA, PGV, peak ground displacement (PGD), I_a (Arias, 1970), and CAV (Electrical Power Research Institute [EPRI], 1988). We have selected I_a and CAV because they are simple and efficient ground-motion parameters to measure the earthquake destructiveness potential. As integral ground-motion parameters, I_a and CAV are influenced by, and therefore reflect, the amplitude, frequency content, and duration of ground motion (Kramer, 1996). Moreover, these parameters can be rapidly computed in real or near-real time at the recording station. The rapid availability of such parameters make them potentially useful for plotting the earthquake ground shaking for a certain region. Herein, the felt intensity is reported in terms of most widely used seismic observed intensity scale—the MMI scale. The motivation behind such correlations has been to extend our knowledge on measuring the earthquake intensity and the earthquake damage potential for the region of Greece.

Data Set

We have gathered strong-motion data, recorded in Greece from 4 November 1973 to 7 September 1999. The strong-motion data are available for download from the Internet (www.isesd.cv.ic.ac.uk, last accessed June 2008) for European strong-motion data (Ambraseys *et al.*, 2004). No additional filtering or correction has been applied to the selected records because they were available in an already-corrected form.

Two orthogonal horizontal components of the recorded motion were used, and it was decided to treat each independently rather than to introduce a vector sum of the two because the maximum values are not realized simultaneously in each component. Therefore, any computed quantities based on summation would be upper bounds of the parameters of interest, thus limiting their practical use (Koliopoulos *et al.*, 1998). Also, most of the existing predictive relations refer to parameters of single components, and the use of the vector sum in the present work would not facilitate any direct comparisons.

Horizontal components with acceleration amplitudes greater than 10 cm/sec^2 were selected and the observed range for the two horizontal components was from about 10 to 515 cm/sec^2. The threshold was chosen because earthquake studies indicate that significant damage does not occur until the acceleration amplitudes exceed the 10 cm/sec^2. The final data set consisted of 310 horizontal components from 89 earthquakes recorded in Greece, and the summary of the selected data set is presented in Table 1.

The earthquake source parameters of interest were the moment magnitude (**M**) and the epicentral depth (H). The data set includes records for small to moderate magnitude events, with **M** ranging from 4 to 6.9. Hypocentral depths of the selected earthquakes are in the interval 0–60 km with a mean of 11.8 km. The recording station parameters that have been considered are epicentral distance (R) and local site geology. Most of the events were offshore and those onshore do not show surface faulting. It was impossible to use a distance-to-fault measure like the closest distance to the fault rupture or to the surface projection of the rupture (Danciu and Tselentis, 2007).

The epicentral distances cover the range from 1 to 124 km. To characterize the near-surface geology at the recording site, a simplified soil classification was accomplished, based on the shear-wave velocity average over the upper 30 m of the site (V_{s30}) reported at the instrument location. The characterization of the local geological conditions is soft soil ($V_{s30} = 200$–360 m/sec)—94 records and average rock ($V_{s30} > 400$ m/sec)—216 records. The distribution of the current data set regarding the local soil classification and the earthquake source parameters—magnitude and epicentral distance—is shown in Figure 1.

Other important properties of the strong ground motion are the duration and frequency content. Among the various duration definitions presented in the literature, we have considered the duration definition proposed by Trifunac and Brady (1975b) and denoted this as significant duration. The significant duration was defined as the time interval over which a percentage (default is the interval between the 5% and 95% thresholds) of the total Arias intensity is accumulated. The significant duration was computed from the acceleration time history, and the distribution histogram of the significant duration for the present data set is presented in Figure 2a. The majority of data have the significant duration concentrated around 8–10 sec.

The frequency characteristic of the motions is investigated with the help of the mean period parameter (T_m) and is illustrated in Figure 2b. T_m utilizes the Fourier amplitude spectrum, averaging periods (over a specified period range) weighted by the Fourier amplitudes, and it was preferred because it better distinguishes the frequency content of strong ground motions (Rathje *et al.*, 2004). The mean period of the selected records is concentrated in the range of 0.2–0.7 sec (i.e., frequency of 1.5–5 Hz). In summary, the present

Table 1
List of the Earthquakes Used for This Study

Earthquake Name	Date (dd/mm/yyyy)	Time (Coordinated Universal Time [UTC])	**M**	$Number_{MMI}$	*R* Range (km)
Ioanian	11/04/1973	15:52:12	5.8	2	≤15
Ioanian	11/04/1973	16:11:36	4.8	2	≤9
Patras	29/01/1974	15:12:43	4.5	2	≤13
Achaia	18/05/1978	00:18:49	4.0	2	≤8
Volvi	20/06/1978	20:03:22	6.2	6	≤26
Volvi	04/07/1978	22:23:28	5.5	2	≤16
Volos	09/07/1980	02:11:55	6.6	2	≤65
Alkion	24/02/1981	20:53:39	6.6	4	19–20
Alkion	25/02/1981	02:35:53	6.3	2	≤25
Preveza	10/03/1981	15:16:20	5.4	4	28–42
Kefallinia Island	17/01/1983	12:41:31	6.9	4	104–124
Kyllini (foreshock)	20/02/1983	05:45:12	4.9	2	≤28
Etolia	16/03/1983	21:19:41	5.3	2	≤16
Kefallinia (aftershock)	23/03/1983	19:04:06	5.2	2	≤11
Kefallinia (aftershock)	23/03/1983	23:51:08	6.2	6	≤72
Off coast of Magion Oros Peninsula	06/08/1983	15:43:53	6.6	2	≤87
Ierissos	26/08/1983	12:52:09	5.1	4	≤7
Near southeast coast of Zakynthos Island	04/10/1984	10:15:12	5.0	2	≤17
Kranidia	25/10/1984	14:38:30	5.5	2	≤23
Kremidia (aftershock)	25/10/1984	09:49:15	5.0	2	≤36
Elis	13/08/1985	13:49:14	4.9	2	≤18
Near coast of Preveza	31/08/1985	06:03:47	5.2	6	13–21
Gulf of Kiparissiakos	07/09/1985	10:20:51	5.4	2	≤37
Drama	09/11/1985	23:30:43	5.2	4	42–104
Skydra–Edessa	18/02/1986	14:34:04	5.3	2	≤31
Peratia	22/05/1986	09:19:53	4.1	2	≤7
Timfristos	14/06/1986	07:40:39	4.0	2	≤8
Timfristos	14/06/1986	09:49:18	4.0	2	≤9
Kalamata	13/09/1986	17:24:34	5.9	4	61–93
Near northwest coast of Kefallinia Island	27/02/1987	23:34:52	5.7	2	≤35
Kalamata (aftershock)	10/06/1987	14:50:12	5.3	2	≤17
Dodecanese	05/10/1987	09:27:02	5.3	2	≤26
Astakos	22/01/1988	06:18:55	5.1	2	≤34
Agrinio	08/03/1988	11:38:57	4.9	2	≤34
Gulf of Corinth	03/04/1988	03:56:07	4.5	2	≤19
Ionian	24/04/1988	10:10:33	4.8	4	12–13
Etolia	18/05/1988	05:17:42	5.3	4	20–23
Etolia	22/05/1988	03:44:15	5.4	2	≤21
Gulf of Corinth	05/07/1988	20:34:52	4.9	2	≤20
Off coast of Levkas Island	24/08/1988	10:10:33	4.5	2	≤14
Kyllini	22/09/1988	12:05:39	5.3	2	≤23
Kyllini	16/10/1988	12:34:05	5.9	8	14–36
Kyllini (aftershock)	20/10/1988	13:32:37	4.2	2	≤13
Trilofon	20/10/1988	14:00:59	4.8	2	≤7
Kyllini (aftershock)	22/10/1988	14:58:18	4.5	4	12–16
Kyllini (aftershock)	23/10/1988	03:17:03	4.3	2	≤7
Kyllini (aftershock)	23/10/1988	07:29:58	4.4	2	≤16
Kyllini (aftershock)	31/10/1988	02:59:51	4.8	2	≤14
Kyllini (aftershock)	27/11/1988	16:38:45	4.5	4	14–19
Patras	22/12/1988	09:56:50	4.9	4	5–21
Patras	15/05/1989	22:40:04	4.8	2	≤6
Patras	31/08/1989	21:29:31	4.8	4	14–21
Aigion	17/05/1990	08:44:06	5.3	2	≤20
Plati	08/08/1990	00:35:07	5.1	2	≤15
Griva	21/12/1990	06:57:43	6.1	4	≤66
Kefallinia Island	23/01/1992	04:24:17	5.6	2	≤43
Mataranga	30/05/1992	18:55:40	5.2	8	23–65
Kefallinia Island	23/06/1992	04:24:17	5.0	2	≤16
Tithorea	18/11/1992	21:10:41	5.9	4	25–63
Levkas Island	10/11/1992	22:14:59	4.6	2	≤5
Gulf of Corinth	04/02/1993	02:22:59	5.3	4	9–11

(*continued*)

Table 1 (*Continued*)

Earthquake Name	Date (dd/mm/yyyy)	Time (Coordinated Universal Time [UTC])	M	Number_{MMI}	R Range (km)
Near coast of Filiatra	05/03/1993	06:55:06	5.2	4	54–57
Pyrgos (foreshock)	26/03/1993	11:45:16	4.9	4	≤1–16
Pyrgos (foreshock)	26/03/1993	11:56:14	4.9	4	≤4–24
Pyrgos	26/03/1993	11:58:15	5.4	4	10–24
Mouzakaiika	13/06/1993	23:26:40	5.3	4	37–48
Pyrgos (aftershock)	10/07/1993	20:26:04	5.1	2	≤21
Patras	14/07/1993	12:31:50	5.6	18	10–54
Patras (aftershock)	14/07/1993	12:39:13	4.6	2	≤11
Gulf of Corinth	04/11/1993	05:18:37	5.3	4	10–19
Komilion	25/02/1994	02:30:50	5.4	10	12–29
Ionian	27/02/1994	22:34:52	4.8	4	14–27
Paliouri	10/04/1994	19:46:21	5.1	2	≤5
Arnaia	04/05/1995	00:34:11	5.3	4	32–43
Kozani	13/05/1995	08:47:15	6.5	12	17–73
Aigion	15/06/1995	00:15:51	6.5	10	12–124
Aigion (aftershock)	25/06/1995	01:05:32	4.1	4	11–12
Kozani (aftershock)	14/05/1995	14:46:57	4.5	2	≤6
Kozani (aftershock)	15/05/1995	04:13:57	5.2	2	≤6
Kozani (aftershock)	16/05/1995	23:57:28	4.9	2	≤27
Kozani (aftershock)	17/05/1995	04:14:25	5.3	2	≤11
Kozani (aftershock)	19/05/1995	06:48:49	5.2	2	≤15
Kozani (aftershock)	06/06/1995	04:36:00	4.8	2	≤11
Kozani (aftershock)	11/06/1995	18:51:48	4.8	4	11–25
Levkas Island	23/04/1996	17:21:49	3.9	2	≤6
Pyrgos	11/08/1996	11:43:45	4.7	2	≤2
Kalamata	13/10/1997	13:39:40	6.4	2	≤61
Strofades	18/11/1997	13:07:41	6.6	2	≤78
Ano Liosia	07/09/1999	11:56:51	6.0	18	14–20
Total number of considered instrumental recordings with MMI observations				310	

M is the moment magnitude, Number_{MMI} is the number of the records with observed or assigned intensity, and *R* is the range of the epicentral distance.

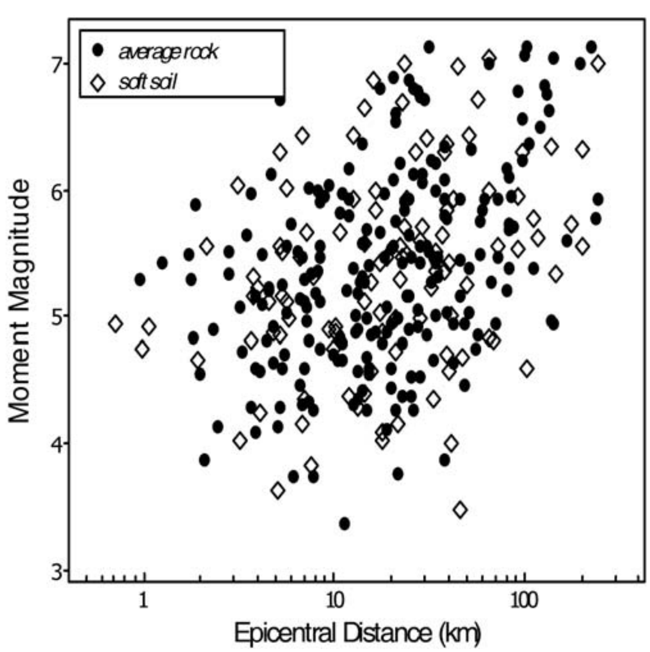

Figure 1. Distribution of the data set with the regard of magnitude, epicentral distance, and local site conditions.

database consists mostly of nonimpulsive records, characterized by high-frequency, low-energy content and short duration.

The macroseismic information associated with each record was provided by the Geodynamic Institute, National Observatory of Athens (GNOA). The institute has been collecting and evaluating macroseismic observations for more than 100 yr, following the questionnaire procedure. The questionnaires are ranked with respect to the MMI scale, and the assessed macroseismic intensities are published in the monthly bulletins. For some earthquakes, the isoseismal maps drawn by an expert's hand are included in the bulletins. Recently, this macroseismic information has been gathered into a macroseismic database developed by Kalogeras *et al.* (2004).

The macroseismic information was available partly from the digital database of the web site for European strong-motion data and was partly estimated separately by us from the macroseismic data provided by the GNOA (Kalogeras *et al.*, 2004). The general criterion was to allocate at each station the nearest MMI values within an uncertainty of one unit to every station. If more than one MMI value was observed near the station location at equal distance, the average of the values was used.

Maps of the reported MMI values together with the strong-motion instrument locations were plotted to obtain

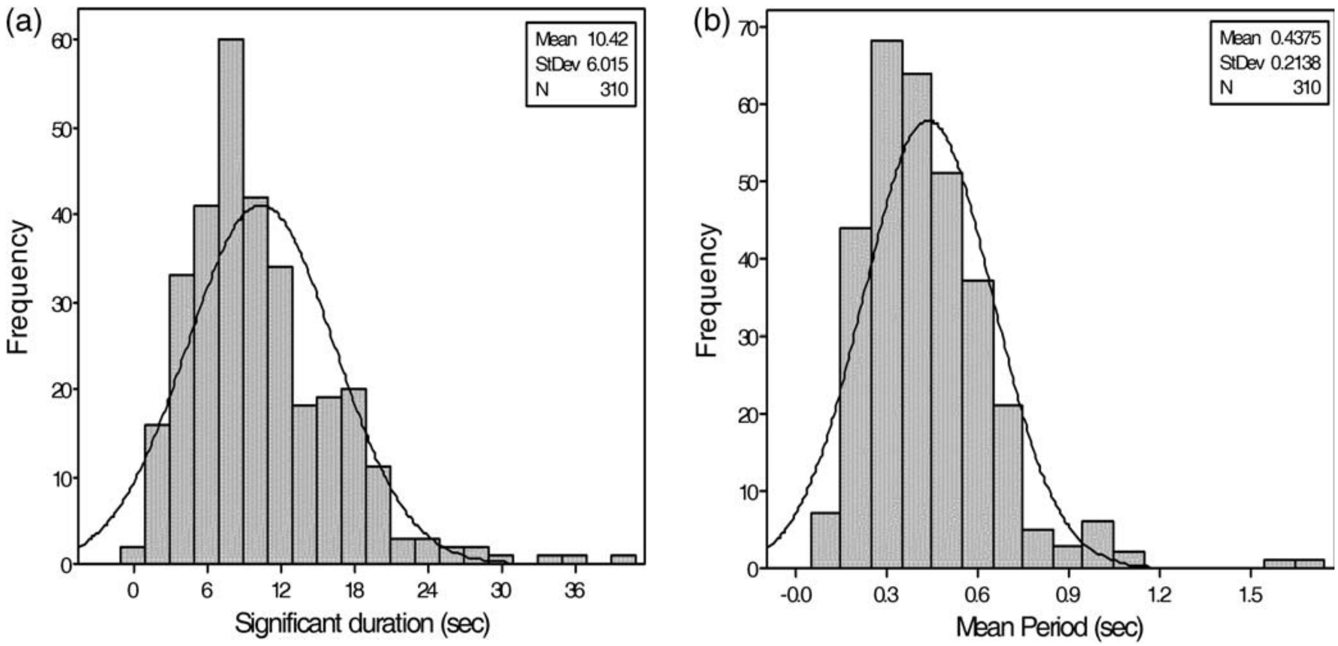

Figure 2. Frequency distribution of the observations considering the significant duration (a) and the mean period (b).

reasonable confidence that the allocated MMI value would be within one unit of the assigned value. This approach provides a rapid visualization of the macroseismic distribution in the area surrounding the recording stations and might be efficient in assigning MMI values to minimize the errors (Atkinson and Kaka, 2007).

This approach is exemplified in Figure 3a, where the reported MMI values for the **M** 6.5 1995 Kozani earthquake are plotted together with the locations of the strong-motion recording instruments. This earthquake occurred in northern Greece and severely damaged about 5000 houses. It was unexpected in the sense that the epicentral region was assumed to be of low seismic risk (Hatzfeld *et al.*, 1997).

It is apparent that the MMI can be assigned with an uncertainty of one-half to one MMI value for most of the stations. For instance, the MMI VII value assigned to the station KOZ was obtained by a simple average from the nearest MMI values observed (e.g., three MMI VII values and one MMI VI value). We note that the volume of the present database was constrained by the limited number of the recording stations in Greece. The distribution of the number of observations in regard to the main sources of assigned MMI values is illustrated in Figure 3b. Moreover, the collected number of MMI values does not cover the low intensity levels from I to IV and the high intensity levels from IX to XII.

Empirical Relationships

The intensity ground-motion parameter relationship is characterized by the large scatter of the observations, the inconsistent distribution of data through the intensity levels, and the subjective nature of the intensity scale (e.g., PGA and PGV data, together with the mean values reported for each MMI level for the two soil categories is plotted in Fig. 4a,b). From this figure, the irregular distribution of data through the MMI levels can be observed. There are few MMI values of VII or VIII and a large number of MMI values of IV or VI. Moreover, it can be observed that, for intensities less than VII, the mean values of the parameters on rock are slightly higher than those on the soft soil.

This amplification observed on rock might appear to be in contradiction with current engineering ideas about the effect of local site conditions on the ground-motion parameters. A similar trend was observed and explained previously by Ambraseys (1974), Trifunac and Brady (1975a), and Murphy and O'Brien (1977). Their explanation was based on wave attenuation and site transfer functions. However, they have shown that the amplification of the motion on the soft soil might occur at certain frequencies even though the peak motion in the time domain is attenuated.

Thus, this amplification of the lower frequency components could be expected to correlate with higher intensity values, and this can be observed at MMI VII, where the mean values of the parameters on soft soil are higher than those on rock. At the first stage of the intensity ground-motion investigation, we have decided not to deaggregate the soil effect, because the soft soil subset comprises only 30% of the total data set. The scatter diagrams of the mean values of the PGA and PGV samples plotted versus MMI presented in Figure 4 reveal a general linear trend, with values of PGA and PGV increasing as MMI increases. Therefore, the expected linear relationship between the dependent (MMI) and independent (ground-motion parameters) variables is

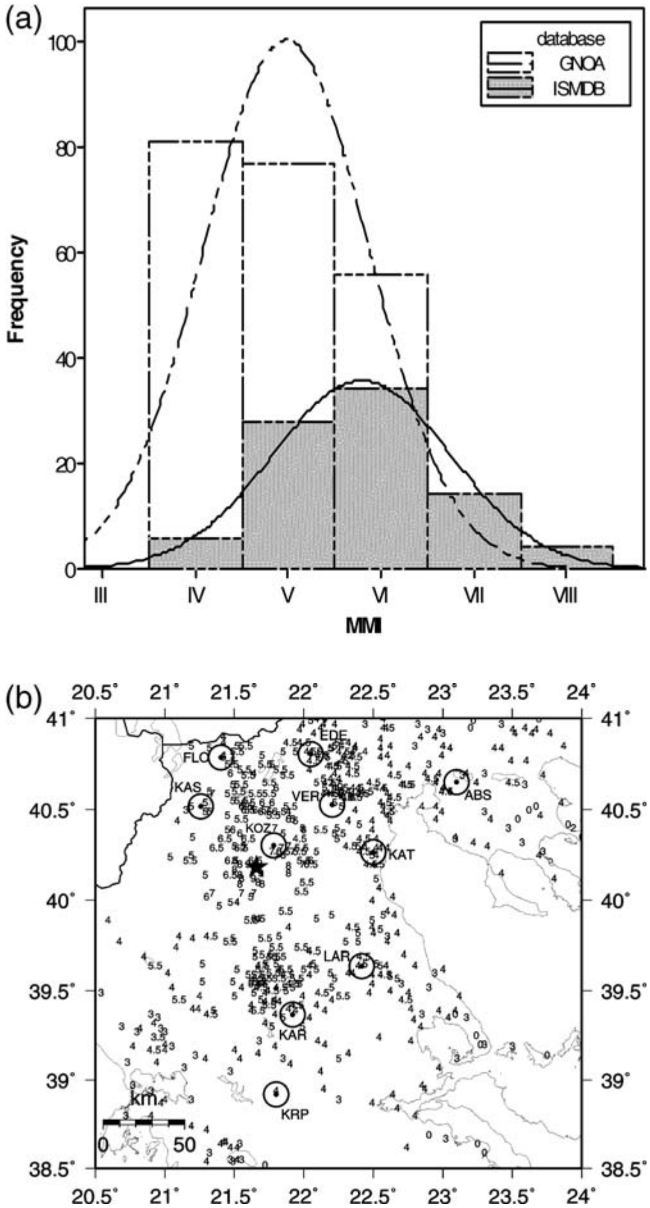

Figure 3. (a) Frequency distribution of the number of MMI observations in regard with the two main sources of macroseismic information: Internet Strong-Motion Database (ISMDB) and Geodynamic National Observatory of Athens (GNOA). (b) Observations for the **M** 6.5 1995 Kozani earthquake. The macroseismic intensity is represented by numbers, and the station locations are plotted together within the area of felt intensity as a dot surrounded by circles. The epicenter is plotted as a black star.

$$\mathrm{MMI}_{(Y)} = b_0 + b_1\overline{\log(Y)} + \varepsilon_{\mathrm{MMI}_{(Y)}}, \qquad (1)$$

where $\overline{(Y)}$ is the average of the ground-motion parameter, b_0 the intercept, b_1 the slope obtained from the linear regression, and $\varepsilon_{\mathrm{MMI}_{(Y)}}$ the error term.

For each MMI level, the mean and the standard deviation of the selected ground-motion parameters were computed assuming a lognormal distribution of the data and are summarized in Table 2. It is important to note that the mean values for the ground-motion parameters were computed from the two orthogonal horizontal components at a site. As it can be observed from the Table 2, the number of observations at each MMI level is not symmetrical. To overcome this shortcoming, weighted linear regression was used to fit, independently of magnitude and/or distance, the dependent (MMI) and the independent (mean values of each ground-motion parameters) variables. The relative weight assigned to each MMI level was based on the number of observations.

The resulting regression coefficients are presented in Table 3, except for PGD. We have excluded this parameter from the regression analysis because of the small mean values, less than 2 cm, observed at low intensity levels. These small values observed at low intensities might be indistinguishable from the recording and processing noise. If these observations at low intensities were removed, then the remaining observations at intensity VII and VIII are not enough to empirically derive a reliable MMI-PGD relationship. Thus, we report the PGD mean values associated with each MMI level, but we do not derive an empirical MMI-PGD relationship.

The standard deviation values associated with the regression model for all parameters reported in Table 3 shows that the scatter is large. These equations cannot predict the expected MMI with a precision of better that about one unit in the case of PGA, one unit and a half for PGV, and I_a or two units in the case of CAV. PGA shows lower variability (smallest standard deviation value $\varepsilon = 0.73$) in predicting MMI. One should bear in mind the present number of observations and the fact that the present database is dominated by high-frequency observations. The large standard deviation values reported for equation (1) suggests a need for improvement of the functional form for the MMI–ground-motion relationship. Figures 5 and 6 illustrate the MMI residuals from equation (1) with respect to the magnitude and distance and the two local soil categories. It can be observed from these figures that the MMI prediction from ground-motion parameters exhibits an apparent dependence on magnitude and epicentral distance. To investigate the significance of these important variables, as well as the effects of the local soil conditions, a more refined functional form of the equation (1) was used:

$$\mathrm{MMI}_{(Y)} = a + b\log_{10}(Y) + m\mathbf{M} + r\log_{10}(R) + sS + \varepsilon_{\mathrm{MMI}_{(Y)}}, \qquad (2)$$

where $\mathrm{MMI}_{(Y)}$ is the MMI predicted from the Y ground-motion parameter, **M** is the moment magnitude, R is the epicentral distance, S is a soil category dummy variable 0 for rock sites and 1 for soft soil sites, a, b, m, r, and s are regression coefficients, and $\varepsilon_{\mathrm{MMI}_{(Y)}}$ is the error term with mean zero and σ equal to 1.

The regression coefficients were obtained from the data set by using multiple linear regression techniques. The statistical significance of each regression coefficient was tested using the t-test. A probability level of 0.05 was chosen to

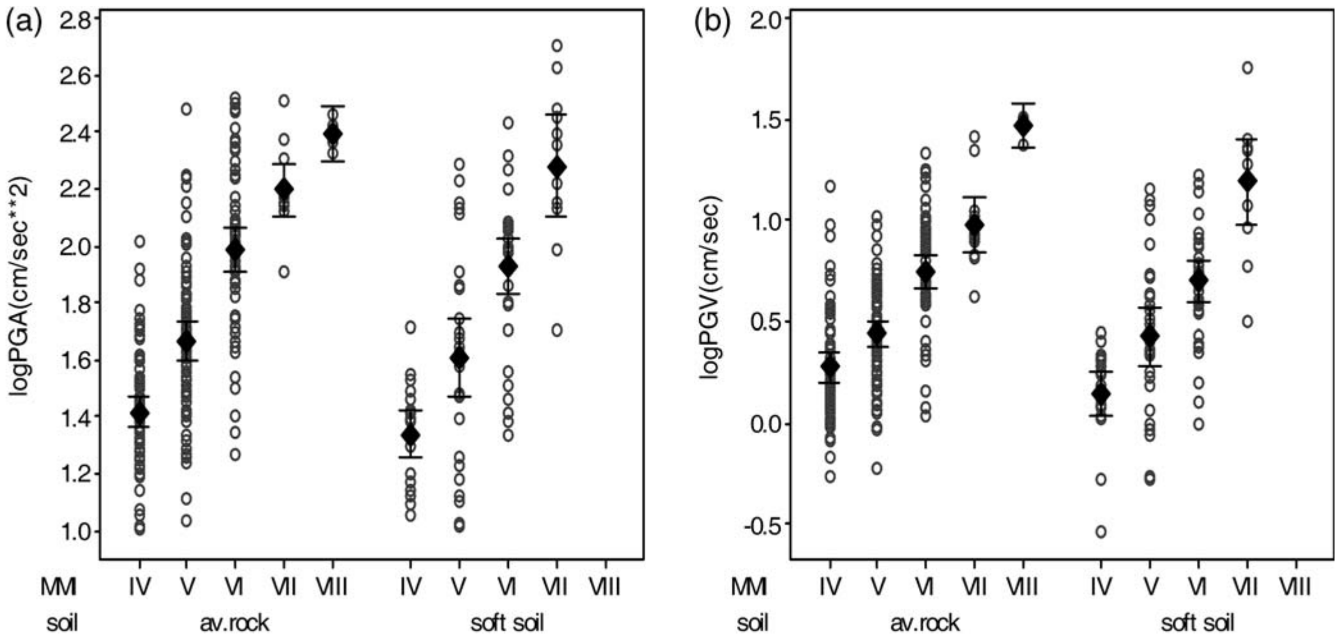

Figure 4. Distribution of the average and standard deviation error bars for (a) log (PGA) and (b) log (PGV) at each intensity levels on soft soil and on average rock.

define the statistical significance, and the results show that the magnitude coefficient, m, is significant only in the case of MMI predicted from PGA. In all of the other cases, the magnitude coefficient m was not significant; thus, the magnitude coefficient was removed from the functional form presented in equation (2). The final form of equation (2) was as follows:

$$\mathrm{MMI}_{(y=\mathrm{PGA})} = a + b\log_{10}(Y) + m\mathbf{M} + r\log_{10}(R) + sS + \varepsilon_{\mathrm{MMI}_{(Y=\mathrm{PGA})}},$$

$$\mathrm{MMI}_{(y=\mathrm{PGA},I_a,\mathrm{CAV})} = a + b\log_{10}(Y) + r\log_{10}(R) + sS + \varepsilon_{\mathrm{MMI}_{(Y=\mathrm{PGV},I_a,\mathrm{CAV})}}. \quad (3)$$

The regression coefficients of equation (3) along with the standard errors for each coefficient are listed in Table 4. Each regression coefficient is statistically significant at a level smaller than 0.05 (p value < 0.05 that the coefficient is equal to zero, using hypothesis testing and the statistical t distribution), except for soil coefficient s for the MMI-PGV relationship. However, we did not remove it due to the fact that the reported p value is small, around 0.077, which means that the coefficient is sufficiently significant to remain in the predictive equation.

A rapid overview of the standard deviation values listed in the Table 4 reveals that the variability in the prediction of the MMI was reduced. The standard deviation values are smaller but still we cannot empirically predict the MMI to better than about one-half to one unit. The smaller standard deviation values are comparable, and the smallest value is observed for I_a (around 0.65).

In Figures 7 and 8, we plot the MMI residuals (observed-predicted) for equation (3) versus magnitude and epicentral distance, respectively. It can be observed that there is no obvious trend between the residuals and the magnitude or distance for both soil categories.

In summary, the MMI prediction from the ground-motion parameters appears to be more significant when other parameters such as magnitude, epicentral distance, and local soil conditions are involved in the predictive model.

Table 2
The Mean and Standard Deviation of Ground-Motion Parameters at Each MMI Level.

MMI	Count	PGA (cm/sec^2)		PGV (cm/sec)		PGD (cm)		I_a (cm/sec)		CAV (cm/s)	
		μ	σ	μ	σ	μ	σ	μ	σ	μ	σ
IV	87	25.04	1.67	1.76	1.90	0.74	2.26	0.75	2.79	63.61	2.00
V	105	44.57	2.04	2.74	2.01	0.80	2.43	1.71	3.42	92.41	2.01
VI	90	92.19	1.95	5.38	2.00	0.92	2.34	5.74	3.38	150.56	1.97
VII	24	173.66	1.68	12.19	1.97	2.18	2.23	24.02	2.35	338.53	1.64
VIII	4	249.17	1.15	29.80	1.17	6.78	1.19	67.89	1.23	522.16	1.11

Table 3
Regression Coefficients of Equation (1) to Predict MMI from the Mean Values of the Ground-Motion Parameters

	Equation (1) $\mathrm{MMI} = b_0 + b_1\overline{\log_{10}(Y)}$		
Ground-Motion Parameters	Regression Coefficients	Values	Standard Error
PGA (cm/sec^2)	b_0	−0.946	0.266
	b_1	3.563	0.153
	$\sigma_{\mathrm{MMI\text{-}PGA}}$	0.734	
PGV (cm/sec)	b_0	3.300	0.199
	b_1	3.358	0.335
	$\sigma_{\mathrm{MMI\text{-}PGV}}$	1.589	
I_a (cm/sec)	b_0	4.395	0.095
	b_1	2.040	0.153
	$\sigma_{\mathrm{MMI\text{-}}I_a}$	1.278	
CAV (cm/sec)	b_0	−3.765	0.987
	b_1	4.406	0.482
	$\sigma_{\mathrm{MMI\text{-}CAV}}$	1.852	

Comparison of the Proposed Relationships with Other Available Relationships

A measure of the agreement between the regression results and the experimental values is provided by comparing the proposed relationships with the other available relationships for the region of interest—Greece. The relationships proposed by Theodulidis and Papazachos (1992) and Koliopoulos *et al.* (1998) are of main interest, and these studies are representative for the region of Greece. In addition, the studies of Margottini *et al.*, 1992 and Cabanas *et al.* (1997) were selected to compare the MMI predicted from the I_a parameter. The comparison among these studies is difficult due to the different number of observations, different assumptions of the functional form of attenuation, and different regression techniques adopted by various authors to fit the data.

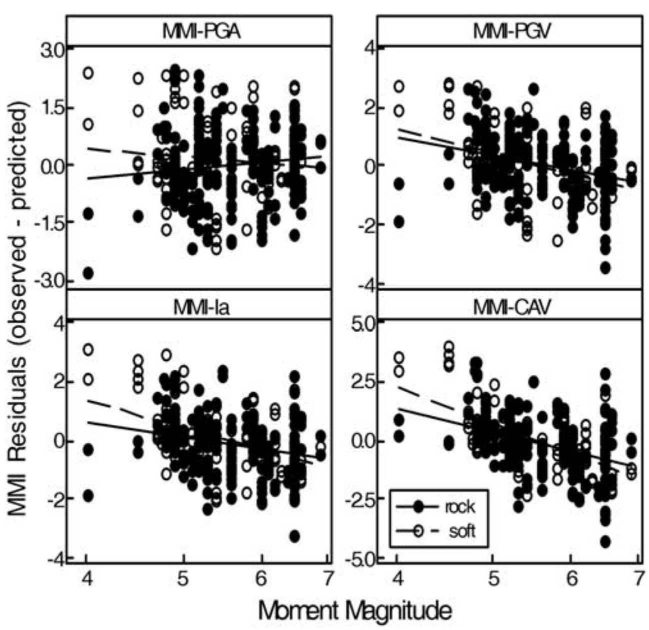

Figure 5. Residuals (observed MMI-predicted MMI) for predicted MMI from the ground-motion parameters using equation (1) for observations on soft soil (empty circles) and average rock (black circles) as a function of moment magnitude.

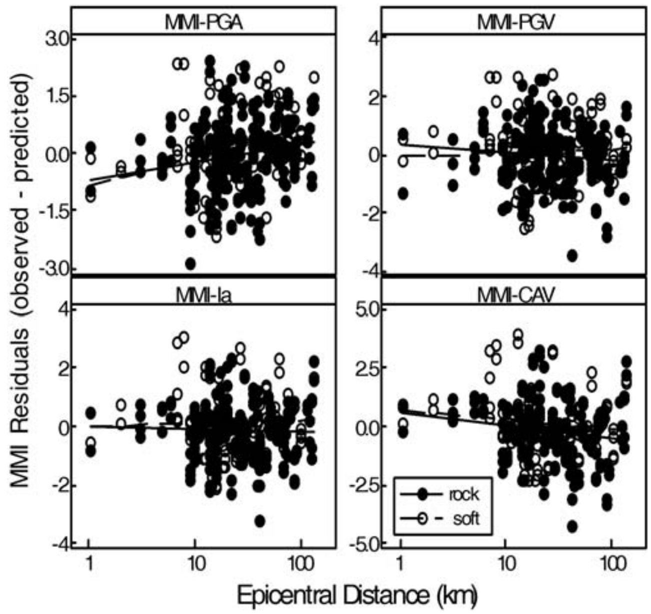

Figure 6. Residuals (observed MMI-predicted MMI) for predicted MMI from the ground-motion parameters using equation (1) for observations on soft soil (empty circles) and average rock (black circles) as a function of epicentral distance.

Theodulidis and Papazachos (1992), using 53 records from Greek earthquakes, derived the relationships over the MMI range of IV–VIII for peak ground-motion parameters. The empirical relationships were obtained by fitting all of the data with a two stage least-squares regression technique.

The influence of the local site condition has also been investigated previously and it was found that at a particular MMI level, the peak acceleration gives higher amplitudes on rock while the MMI-PGV relationship was found to be independent of the soil conditions. It is interesting to note that these results are in good agreement with the findings presented in the current study. The study of Koliopoulos *et al.* (1998) proposed predictive relationships for MMI and various ground-motion parameters, valid for the intensity range IV ≤ MMI ≤ VI+ when mean values are used and suitable for the interval III ≤ MMI ≤ VIII+ when the total number of observations were considered.

However, for comparison, we have selected the empirical relationships derived from the total number of observations, because we did not want to extrapolate the MMI over the interval IV–VIII. The majority of the observations under consideration (140 out of 201) were classified as alluvium. A simple linear regression was employed by previous authors to fit the mean and the total number of the observations versus the MMI. Margottini *et al.* (1992) conducted a correlation between the macroseismic intensity and PGA and I_a. The data set consisted of 56 records derived from nine Italian earthquakes that occurred between 1980 and 1990.

Table 4
Regression Coefficients of Equation (3) for Predicting MMI from Ground-Motion Parameters (All Data)

Ground-Motion Parameters	$\mathrm{MMI}_{(y=\mathrm{PGA})} = a + b\log_{10}(Y) + m\mathbf{M} + r\log_{10}(R) + sS + \varepsilon$ $\mathrm{MMI}_{(y=\mathrm{PGV},I_a,\mathrm{CAV})} = a + b\log_{10}(Y) + r\log_{10}(R) + sS + \varepsilon,$				
	Regression Coefficients	Values	Standard Error	t	p Value
PGA (cm/sec^2)	a	2.355	0.383	6.142	0.000
	b	1.384	0.123	11.220	0.000
	m	0.297	0.084	3.537	0.000
	r	−0.832	0.157	−5.309	0.000
	s	−0.108	0.041	−2.625	0.009
	$\sigma_{\mathrm{MMI\text{-}PGA}}$	0.666			
PGV (cm/sec)	a	5.582	0.167	33.372	0.000
	b	1.397	0.099	14.056	0.000
	r	−0.787	0.100	−7.880	0.000
	s	−0.073	0.041	−1.777	0.077
	$\sigma_{\mathrm{MMI\text{-}PGV}}$	0.661			
I_a (cm/sec)	a	5.919	0.151	39.180	0.000
	b	0.844	0.057	14.707	0.000
	r	−0.997	0.099	−7.309	0.000
	s	−0.105	0.040	−2.614	0.009
	$\sigma_{\mathrm{MMI\text{-}Ia}}$	0.649			
CAV (cm/sec)	a	3.763	0.280	13.424	0.000
	b	1.409	0.108	13.073	0.000
	r	−0.997	0.099	−10.066	0.000
	s	−0.105	0.042	2.496	0.013
	$\sigma_{\mathrm{MMI\text{-}CAV}}$	0.679			

The intensity data were determined using two approaches: local intensity and general intensity. The separation of the local site conditions has proven to be of practically no influence on the subsequently developed relationships. The data were fitted with a simple linear regression, considering the mean values of the ground-motion parameters. The study of Cabanas *et al.* (1997) was focused on the study of correlation between two macroseismic parameters—local site intensity and observed damage—and two instrumental parameters obtained from strong-

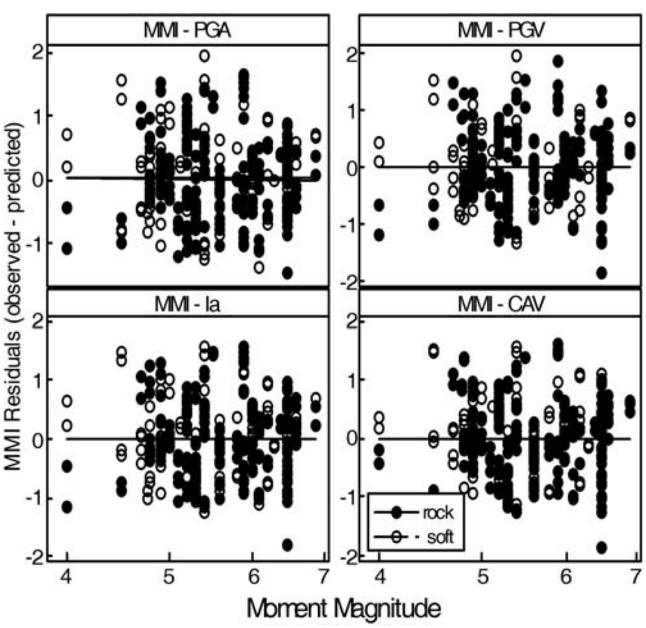

Figure 7. Residuals (observed MMI-predicted MMI) for predicted MMI from the ground-motion parameters using equation (3) for observations on soft soil (empty circles) and average rock (black circles) as a function of moment magnitude.

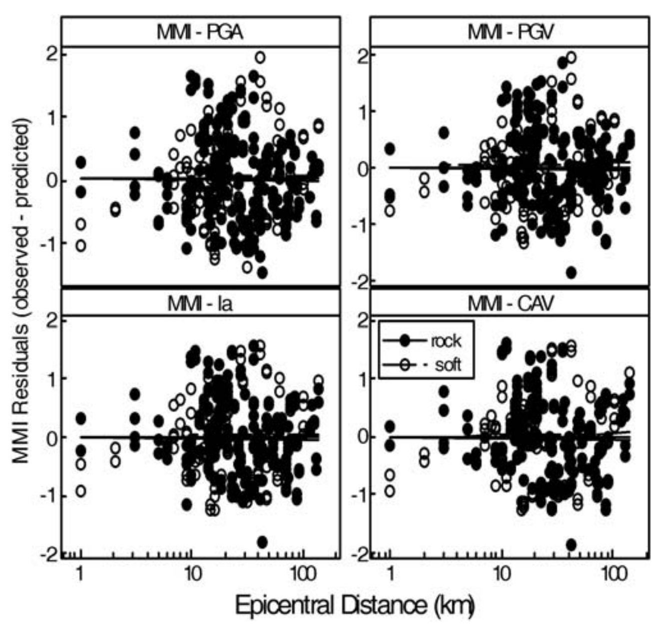

Figure 8. Residuals (observed MMI-predicted MMI) for predicted MMI from the ground-motion parameters using equation (3) for observations on soft soil (empty circles) and average rock (black circles) as a function of epicentral distance.

motion records: I_a and CAV computed for five different thresholds. The study does not take into account the local soil conditions, the I_a and CAV mean values were fitted with a simple linear regression, and the data set consisted of 50 records. Keeping in mind the differences in terms of the earthquake locations, the number of observations, the range of intensities, the ground-motion parameters, the local soil condition, and the statistical technique to fit data that exist between the present study and the previously described studies, the graphical comparison of these relationships is presented in Figures 9–12.

Figure 9 shows the comparison between the present MMI-PGA empirical relationship with those proposed by Theodulidis and Papazachos (1992) and Koliopoulos *et al.* (1998). This comparison shows that the slope of the present empirical MMI-PGA relationship is in good agreement with the relationships proposed by Theodulidis and Papazachos (1992). The slopes are almost parallel, but with lower PGA values for given intensities on rock local soil category and higher PGA values on alluvium. This difference might be explained by the fact that we have not treated the rock or the alluvium sites separately. Also, the number of the observations as well as the uneven distribution of these observations at each MMI level, together with the different regression techniques involved (weighted least-squares regression, two stage least-squares regression, simple least-squares regression) in fitting the data, might partially explain these differences. Figure 10 illustrates the comparison of the present MMI-PGA relationship with those selected for comparison. With reference to this figure, it can be seen that our predictive equations give higher PGV values than the relationships proposed by Theodulidis and Papazachos (1992). For low intensity levels, our predictive model provides the highest PGV values, and then the values are attenuated as the intensity is increased. This could partially be attributed, as in the case of PGA, to differences in the distribution of the observations regarding the local soil conditions and the distribution at each MMI level. Nevertheless, the compared relationships were obtained by fitting the total number of observations, whereas the present relationships were obtained by fitting the MMI versus the mean values of the ground-motion parameters.

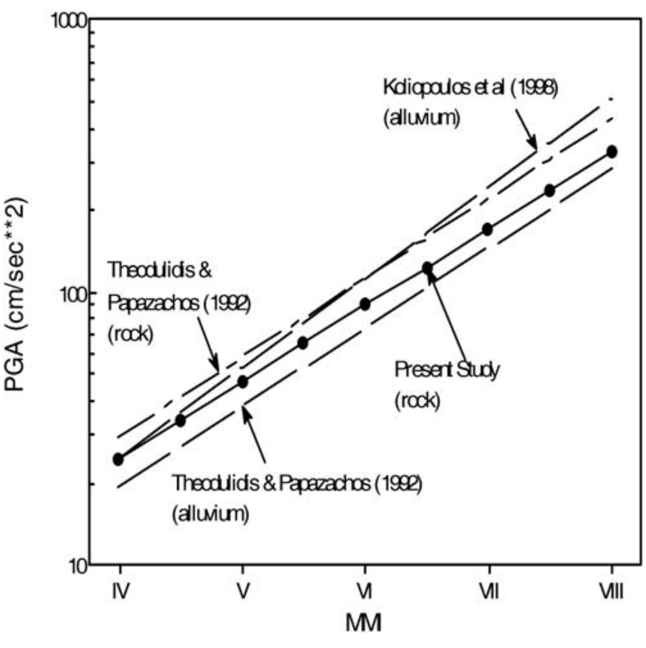

Figure 9. Comparison of the empirical relationships proposed for predicting MMI from the mean values of PGA with equation (1) with similar relationships proposed by other studies.

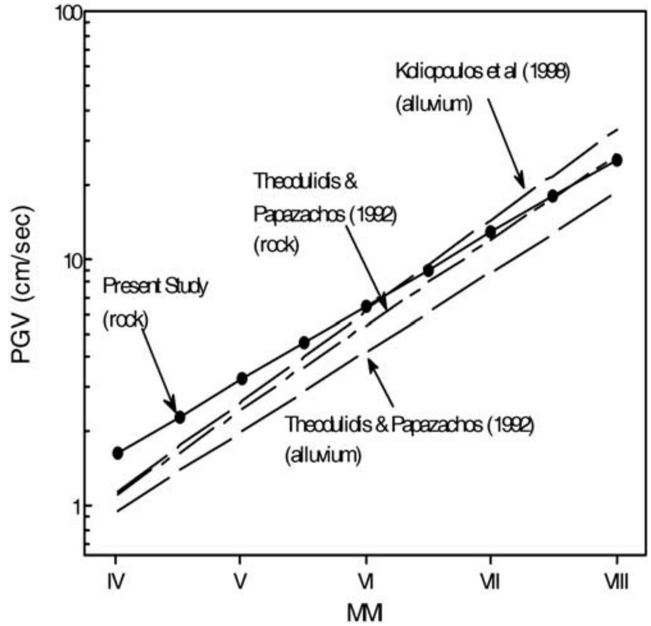

Figure 10. Comparison of the empirical relationships proposed for predicting MMI from the mean values of PGV with equation (1) with similar relationships proposed by other studies.

Differences between the predicted MMI from I_a provided by the selected studies can be observed in Figure 11. The present empirical model predicts I_a values smaller than those derived on the other studies. The tendency of slope corresponding to the present MMI-I_a relationships is slightly different than the one proposed by Koliopoulos *et al.* (1998). As can be seen in Figure 11, the proposed MMI-CAV relationship exhibits a similar trend with the relationship proposed by Koliopoulos *et al.* (1998), the lines are almost parallel, and the present relationship exhibits higher values. However, these differences are difficult to explain because, apart from the different ground-motion data set used, the definition of the MMI scale might introduce some scatter, although it is declared as modified Mercalli in all of the studies (Theodulidis and Papazachos, 1994).

In earthquake engineering practice, the MMI VI is considered a conservative reference point for earthquake damage, with the reasonable engineering assurance that no damages will occur to buildings of good design and construction. It has been reported that earthquakes in Greece cause damage (MMI > VI) when PGA exceeds 90 cm/sec^2

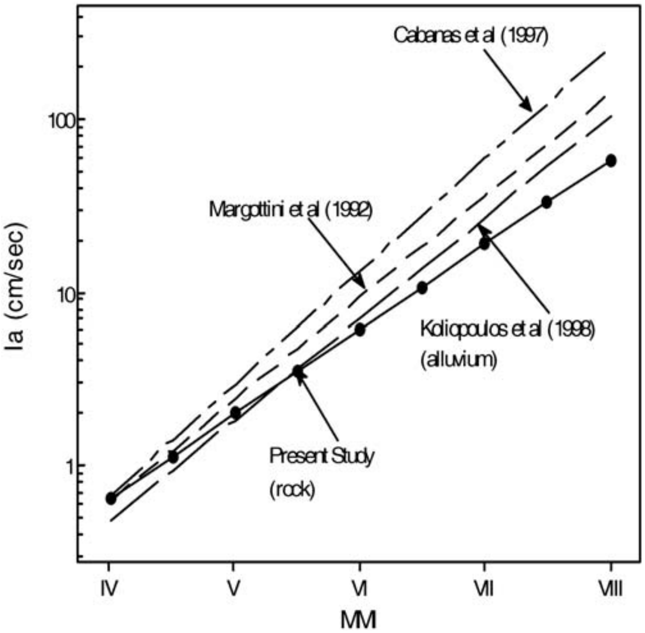

Figure 11. Comparison of the empirical relationships proposed for predicting MMI from the mean values of I_a with equation (1) with similar relationships proposed by other studies.

and PGV exceeds the value of 5 cm/sec (Papazachos and Papazachou, 1997). The PGA and PGV values associated with MMI VI predicted in this study are in good agreement with these values, equal to 89 and 6.5 cm/sec^2, respectively.

Moreover, the CAV value established to determine whether the operating basis earthquake (OBE) has been exceeded after the occurrence of a seismic event at a nuclear power plant (Reed and Kassawara, 1990) was found to be equal to 300 cm/sec. This threshold was obtained in a conservative way and corresponds to a lower limit of the MMI VII. Indeed, the present MMI-CAV relationship predicts a CAV value associated to the MMI VII equal to 277 cm/sec.

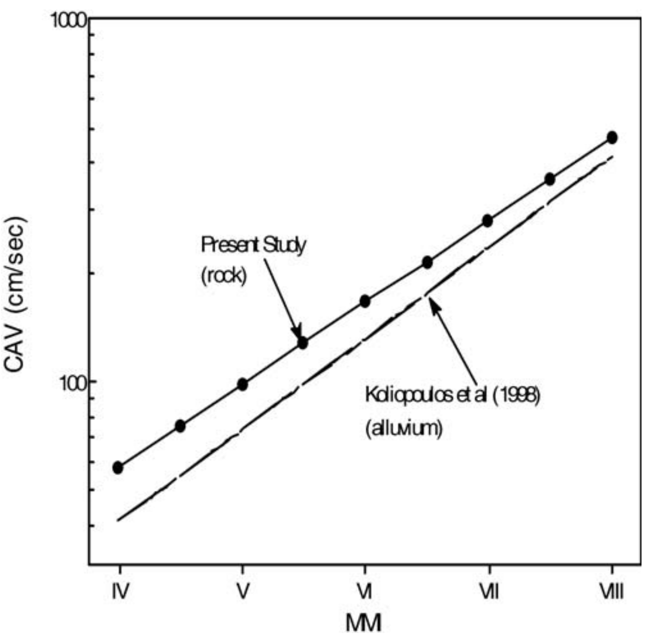

Figure 12. Comparison of the empirical relationships proposed for predicting MMI from the mean values of CAV with equation (1) with similar relationships proposed by other studies.

The present study reports for MMI VII a value of I_a equal to 19 cm/sec, which is in the good agreement with the I_a value (20 cm/sec for MMI VI–VII) observed by Perkins (1998) for San Francisco Bay area. The slight difference between these values might be partly due to the differences between the Greek and American records and due to the inherent statistical variability in the intensity ground-motion relationship. In summary, due to the large amount of data used, it can be concluded that the proposed predictive relationships for MMI from various ground-motion parameters can be accepted as an update of the relationships proposed by Theodulidis and Papazachos (1992) and Koliopoulos *et al.* (1998).

Conclusions

The present study investigates the relationships between various ground-motion parameters and earthquake intensity—quantified by MMI for Greece. The data set contains time history records and macroseismic observations from earthquakes recorded in Greece from 4 November 1973 to 7 September 1999. Two predictive models were used to estimate the MMI from the selected ground-motion parameters. One was based on the mean ground-motion values observed at each MMI level, described by equation (1), and the other was based on the whole data, described by equation (3).

The scatter associated with the MMI prediction from mean values was large and the uncertainty of the MMI prediction was within one to two units in most cases. The model was obtained independent of the magnitude and epicentral distance. If the magnitude and epicentral distances are known, then the second model may be used. The variability in MMI prediction associated to the second predictive model was reduced and the uncertainty of the MMI prediction might be within one-half to one unit.

The lowest standard deviation observed for the first model was observed for PGA, while for the second predictive model, the I_a exhibited the lowest variability. PGA and I_a are well recognized to reflect the higher frequency components of a ground motion. The local site effect was taken into account by incorporating a dummy variable accordingly to the soil classification. It was found that the current classification on rock and soft soil has a very little influence on the prediction MMI from PGV.

The dependence of the magnitude and epicentral distance was investigated for each ground-motion parameter, and it was observed that the predictive MMI from PGA is dependent on both magnitude and epicentral distance. For the other parameters, the magnitude influence was found not to be statistically significant, and thus was not incorporated in the predictive model.

The data are characterized by high-frequency, low-energy, short-duration, nonimpulsive records. The prediction of MMI from PGA is affected by magnitude and epicentral distance, while the MMI prediction from PGV, I_a, or CAV is affected by epicentral distance. The study recommends the use of I_a or CAV for rapid damage assessment tools like ShakeMap. Regardless of that application, the availability of such relationships for a specific region provides a direct link between earthquake hazard evaluation and assessment of the historical earthquakes for which no instrumental data are available. We emphasize that these relationships should be used with care, due to the inherent statistical variability in predicting MMI such that the results cannot be better than about one-half to one unit for a site or event.

Acknowledgments

The cooperation of I. Kalogeras is acknowledged for providing the database of the earthquake records together with the macroseismic information. We thank Tim Sokos at Patras Seismological Laboratory for his help during the data processing. The manuscript was substantially improved with excellent review comments by M. C. Chapman and two anonymous reviewers. This research was supported by the Greek State Scholarship's Foundation (IKY) and, in part, by the 3HAZ-CORINTH EC Project Number 4043.

References

Ambraseys, N. (1974). The correlation of intensity with ground motions, *Proc. of the 14th Conf. of the European Seismological Commission*, Trieste, Italy.

Ambraseys, N., P. Smit, J. Douglas, B. Margaris, R. Sigbjornsson, S. Olafsson, P. Suhadolc, and G. Costa (2004). Internet-site for European strong-motion data, *Boll. Geofis. Teor. Appl.* **45,** no. 3, 113–129.

Arias, A. (1970). *A Measure of Earthquake Intensity*, MIT Press, Cambridge, Massachusetts.

Atkinson, G. M., and S. I. Kaka (2007). Relationship between felt intensity and instrumental ground motion in the central United States and California, *Bull. Seismol. Soc. Am.* **97,** no. 2, 497–510.

Cabanas, L., B. Benito, and M. Herraiz (1997). An approach to the measurement of the potential structural damage of earthquake ground motions, *Earthq. Eng. Struct. Dyn.* **26,** 79–92.

Danciu, L., and G. A. Tselentis (2007). Engineering ground-motion parameters attenuation relationships for Greece, *Bull. Seismol. Soc. Am.* **97,** no. 1B, 162–183.

Electrical Power Research Institute (EPRI) (1988). EPRI Report NP-5930, A criterion for determining exceedance of the operating basis earthquake, Electrical Power Research Institute, Palo Alto, California.

Gutenberg, B., and C. F. Richter (1956). Earthquake magnitude, intensity, energy, and acceleration, *Bull. Seismol. Soc. Am.* **46,** no. 2, 105–145.

Hatzfeld, D., V. Karakostas, M. Ziazia, G. Selvaggi, S. Laborgne, C. Berge, R. Guiguet, A. Paul, P. Voidomatis, D. Diagourtas, I. Kassaras, I. Koutsikos, K. Makropoulos, R. Azzara, M. Di Bona, P. Bernard, and C. Papaioannou (1997). The Kozani-Greven (Greece) Earthquake of 13 May 1995 revised from a detailed seismological study, *Bull. Seismol. Soc. Am.* **87,** no. 2, 463–473.

Hershberger, J. (1956). A comparison of earthquake accelerations with intensity ratings, *Bull. Seismol. Soc. Am.* **46,** no. 4, 317–320.

Kaka, S. I., and G. M. Atkinson (2004). Relationships between instrumental ground-motion parameters and modified Mercalli intensity in eastern North America, *Bull. Seismol. Soc. Am.* **94,** no. 5, 1728–1736.

Kaka, S. I., and G. M. Atkinson (2007). Relationships between felt intensity and instrumental ground motion in the central United States and California, *Bull. Seismol. Soc. Am.* **97,** no. 2, 497–510.

Kalogeras, I. S., G. Marketos, and Y. Theodoridis (2004). A tool for collecting, querying, and mining macroseismic data, *Bull. Geol. Soc. Greece* **36,** no. 3, 1406–1411.

Karim, K. R., and R. Yamazaki (2002). Correlation of JMA instrumental seismic intensity with strong motion parameters, *Earthq. Eng. Struct, Dyn.* **31,** no. 5, 1191–1212.

Koliopoulos, P. K., B. N. Margaris, and N. S. Klims (1998). Duration and energy characteristics of Greek strong motion records, *J. Earthq. Eng.* 391–417.

Kostov, M. K. (2005). Site specific estimation of cumulative absolute velocity, *18th International Conference on Structural Mechanics in Reactor Technology*, Beijing, China.

Kramer, S. L. (1996). *Geotechnical Earthquake Engineering*, Prentice Hall, New York.

Krinitzsky, E. L., and F. K. Chang (1988). Intensity-related earthquake ground motion, *Bull. Int. Assoc. Eng. Geol.* **4,** 425–435.

Margottini, C., D. Molin, and L. Serva (1992). Intensity versus ground motion: a new approach using Italian data, *Eng. Geol.* **33,** 45–58.

McCann, M. W., F. Sauter, and H. C. Shah (1980). A technical note on PGA-intensity relations with applications to damage estimation, *Bull. Seismol. Soc. Am.* **70,** no. 2, 631–637.

Murphy, J. R., and L. J O'Brien (1977). The correlation of peak ground acceleration amplitude with seismic intensity and other physical parameters, *Bull. Seismol. Soc. Am.* **67,** 877–915.

Panza, G. F., R. Cazzaro, and F. Vaccari (1997). Correlation between macroseismic intensities and seismic ground motion parameters, *Ann. Geofis.* **40,** no. 5, 1371–1382.

Papazachos, B., and C. Papazachou (1997). *The Earthquakes of Greece*, Ziti and Company, Thessaloniki, Greece.

Perkins, J. B. (1998). On shaky ground—supplement, *A Guide to Assessing Impacts of Future Earthquakes Using Ground Shaking Hazard Maps for the San Francisco Bay Area*, Association of Bay Area Governments (ABAG), Oakland, California.

Rathje, E. M., F. Faraj, S. Russell, and J. B. Bray (2004). Empirical relationships for frequency content parameters of earthquake ground motions, *Earthq. Spectra* **20,** no. 1, 119–144.

Reed, R. W., and R. P. Kassawara (1990). A criterion for determining exceedance of the operating basis earthquake, *Nucl. Eng. Des.* **123,** 387–396.

Sokolov, V. Y. (1998). Seismic intensity and Fourier acceleration spectra, *Earthq. Spectra* **14,** no. 4, 679–694.

Sokolov, V. Y. (2002). Seismic intensity and Fourier acceleration spectra: revised relationship, *Earthq. Spectra* **18,** no. 1, 161–187.

Theodulidis, N. P., and B. C. Papazachos (1992). Dependence of strong ground motion on magnitude-distance, site geology and macroseismic intensity for shallow earthquakes in Greece: I, peak horizontal acceleration, velocity and displacement, *Soil Dyn. Earthq. Eng.* **11,** 387–402.

Theodulidis, N. P., and B. C. Papazachos (1994). Dependence of strong ground motion on magnitude-distance, site geology and macroseismic intensity for shallow earthquakes in Greece: II, horizontal pseudovelocity, *Soil Dyn. Earthq. Eng.* **13,** 317–343.

Trifunac, M. D., and A. G. Brady (1975a). On the correlation of seismic intensity with peaks of recorded ground motion, *Bull. Seismol. Soc. Am.* **65,** 139–162.

Trifunac, M. D., and A. G. Brady (1975b). A study on the duration of strong earthquake ground motion, *Bull. Seismol. Soc. Am.* **65,** no. 3, 581–626.

Trifunac, M. D., and B. Westermo (1977). A note on the correlation of frequency-dependent duration of strong earthquake ground motion with the modified Mercalli intensity and the geologic conditions at the recording stations, *Bull. Seismol. Soc. Am.* **67,** no. 3, 917–927.

Wald, D. J., V. Quitoriano, T. H. Heaton, and H. Kanamori (1999). Relationships between peak ground acceleration, peak ground velocity, and modified Mercalli intensity in California, *Earthq. Spectra* **15,** no. 3 557–564.

Wald, D. J., V. Quintoriano, T. H. Heaton, H. Kanamori, C. W. Scrivner, and C. B. Worden (1999). TriNet "ShakeMaps": rapid generation of peak ground motion and intensity maps for earthquakes in southern California, *Earthq. Spectra* **15,** no. 3, 537–555.

Wu, Y. M., T. I. Teng, T. C. Shin, and N. C. Hsiao (2003). Relationship between peak ground acceleration, peak ground velocity and intensity in Taiwan, *Bull. Seismol. Soc. Am.* **93,** 386–396.

Seismological Laboratory
Department of Geology
University of Patras
Patras 26500, Greece

Manuscript received 5 July 2007